RESEARCH ARTICLE

BolA Is a Transcriptional Switch That Turns Off Motility and Turns On Biofilm Development

Clémentine Dressaire,[a] Ricardo Neves Moreira,[a] Susana Barahona,[a] António Pedro Alves de Matos,[b] Cecília Maria Arraiano[a]

Instituto de Tecnologia Química e Biológica António Xavier, Universidade Nova de Lisboa, Oeiras, Portugal[a]; Egas Moniz—Cooperativa de Ensino Superior, CRL, Campus Universitário, Quinta da Granja, Monte de Caparica, Caparica, Portugal[b]

C.D. and R.N.M. contributed equally to this work.

ABSTRACT **Bacteria are extremely versatile organisms that rapidly adapt to changing environments. When bacterial cells switch from planktonic growth to biofilm, flagellum formation is turned off and the production of fimbriae and extracellular polysaccharides is switched on. BolA is present in most Gram-negative bacteria, and homologues can be found from proteobacteria to eukaryotes. Here, we show that BolA is a new bacterial transcription factor that modulates the switch from a planktonic to a sessile lifestyle. It negatively modulates flagellar biosynthesis and swimming capacity in *Escherichia coli*. Furthermore, BolA overexpression favors biofilm formation, involving the production of fimbria-like adhesins and curli. Our results also demonstrate that BolA is a protein with high affinity to DNA and is able to regulate many genes on a genome-wide scale. Moreover, we show that the most significant targets of this protein involve a complex network of genes encoding proteins related to biofilm development. Herein, we propose that BolA is a motile/adhesive transcriptional switch, specifically involved in the transition between the planktonic and the attachment stage of biofilm formation.**

IMPORTANCE ***Escherichia coli*** **cells possess several mechanisms to cope with stresses. BolA has been described as a protein important for survival in late stages of bacterial growth and under harsh environmental conditions. BolA-like proteins are widely conserved from prokaryotes to eukaryotes. Although their exact function is not fully established at the molecular level, they seem to be involved in cell proliferation or cell cycle regulation. Here, we unraveled the role of BolA in biofilm development and bacterial motility. Our work suggests that BolA actively contributes to the decision of bacteria to arrest flagellar production and initiate the attachment to form structured communities, such as biofilms. The molecular studies of different lifestyles coupled with the comprehension of the BolA functions may be an important step for future perspectives, with health care and biotechnology applications.**

Received 20 November 2014 **Accepted** 31 December 2014 **Published** 17 February 2015

Citation Dressaire C, Moreira RN, Barahona S, Alves de Matos AP, Arraiano CM. 2015. BolA is a transcriptional switch that turns off motility and turns on biofilm development. mBio 6(1):e02352-14. doi:10.1128/mBio.02352-14.

Editor Susan Gottesman, National Cancer Institute

Address correspondence to Cecília Maria Arraiano, cecilia@itqb.unl.pt.

This article is a direct contribution from a Fellow of the American Academy of Microbiology.

Cellular stress can induce substantial physiological and molecular adaptations to ensure survival. The *bolA* gene is widespread in nature and was initially characterized in *Escherichia coli* as a stationary-phase gene that promotes round morphology when overexpressed (1). Later, it was shown that BolA can also be induced during early growth phase if cells are challenged by several forms of stress, such as heat shock, acidic stress, oxidative stress, and sudden carbon starvation (2). In addition, BolA modulates cell permeability (3) and is involved in biofilm formation not only in *E. coli* (4, 5) but also in *Pseudomonas fluorescens* (6). Interestingly, the heterologous expression of the microalgae *Chlamydomonas reinhardtii* BolA in *E. coli* also favors the development of biofilms (7). Biofilm-associated cells display increased resistance to many toxic substances, such as antibiotics and detergents; this is also observed when *bolA* is overexpressed (3).

The expression of *bolA* is tightly controlled. It is regulated both at the transcriptional and posttranscriptional levels (8–11). In optimal growth conditions, *bolA* transcription is under the control of the housekeeping sigma factor σ^{70}, but in stationary phase or under stress, *bolA* is preferentially transcribed in the presence of sigma factor σ^{s} (2, 11). Direct binding of H-NS or phosphorylated OmpR to the promoter region of *bolA* was shown to repress its expression (12, 13). The posttranscriptional regulation of *bolA* mRNA levels involves both RNase III and poly(A) polymerase (PAPI) (10, 14).

BolA-induced alterations in cell morphology are mediated by a complex network that integrates PBP5, PBP6, and MreB (3, 15–17). BolA was shown to interact with the promoter region of *dacA*, *dacC*, and *mreB* (16, 17). This protein is also involved in the regulation of OmpF/OmpC balance, changing bacterial permeability (3).

Surprisingly, an overall picture of the specific targets and global effects of BolA is still missing. In this report, we demonstrate by chromatin immunoprecipitation sequencing (ChIP-seq) that

BolA is indeed a new transcription factor that directly binds to the promoter region of a number of important genes. Complementing the ChIP-seq experiments with transcriptomic analysis gave a complete overview of the BolA regulatory network and its relevant effects on gene expression. The expression analyses were supported by *in vivo* and *in vitro* phenotypic results, showing that BolA regulates flagellar and curli biosynthesis pathways. Together, our results unravel the mechanism of action of BolA. They explain many of its pleiotropic effects and give new evidence on the impact of BolA in cell motility, significantly affecting flagellar and curli biosynthesis pathways. This involves the downregulation of the master regulator FlhDC coupled with the synthesis of curli and fimbriae and the increased production of the biofilm matrix. These results provide an important advance in the functional characterization of the BolA protein, unraveling its determinant role in the coordination of the flagellar biogenesis and biofilm formation. Therefore, this study is of utmost importance for the comprehension of genetic and molecular bases involved in the regulation of cell motility and biofilm formation and may contribute to future industrial and public health care applications.

RESULTS

Global effects of BolA in bacterial growth. BolA has been described as a pleiotropic protein with influence on cell division and stress response mechanisms (18). Transcriptome analysis was performed to evaluate the impact of BolA in global transcriptional regulation. An *E. coli* MG1655 *bolA* deletion strain (Δ*bolA* strain) carrying an inducible pBAD24 plasmid was compared with the same strain in which *bolA* was cloned in the same plasmid (strain overexpressing BolA [*bolA*++ strain]). The aim of the experimental conditions selected was to stress the effect of BolA in the cell, comparing the absence of BolA and the excess of this protein. The transcriptomic comparison was carried out in exponential (1 h of induction) and stationary (3 h of induction) phases of growth. Both strains were grown in strictly identical conditions and displayed similar growth profiles (see Fig. S1A in the supplemental material). BolA overexpression was confirmed by the typical round morphology adopted by the *E. coli* cells in the presence of elevated levels of this protein (see Fig. S1B). This typical bacterial shape was first observed 40 min after induction of *bolA* expression. As previously described for *bolA* overexpression in the MG1693 background, the spheres slowly increased in size (16) but remained stable, with similar size and shape, for up to 4 h after induction (data not shown). Upon induction, the *bolA*++ strain displayed slightly higher optical density (OD) values than the isogenic control strain, a phenomenon most probably linked with the changes in morphology.

An overview of the results obtained in the transcriptome is given by the volcano plots of Fig. 1A. Comparison of the Δ*bolA* and *bolA*++ strains revealed that the expression of 6% and 46% of *E. coli* genes present in this analysis was significantly differentially regulated 1 h and 3 h after *bolA* induction, respectively. This corresponds to 234 and 1,872 genes with differential expression 1 h and 3 h after induction with arabinose. In order to validate the results, the expression of several of these genes was further analyzed by reverse transcription RT-PCR (see Fig. S2A). Seven different targets were selected for analysis, including genes differentially regulated in the different time points referenced above. All showed to be regulated in the same manner as in transcriptomic analyses.

The genes differentially expressed are almost equally distributed between upregulated and downregulated. Hypergeometric tests were performed on the groups of genes significantly upregulated or downregulated. Due to the redundancy of Gene Ontology (GO) and Kyoto Encyclopedia of Genes and Genomes (KEGG) analyses, only the results associated with the term "biological process of GO classification" are represented (Fig. 1B and C).

bolA is known to be induced by several stress conditions (2, 9, 11). It is thus interesting to observe that upon *bolA* induction, several specific stress response-associated genes are upregulated, including the cold shock proteins *cspI*, *cspB*, *cspG*, *cspH*, *cspC*, *cspF* or *rdoA*, *cpx*, *spy*, and *cpxP*. However, several universal stress proteins (*uspB*, *uspD*, *uspE*, *uspG*) are downregulated under these conditions. BolA also influences the expression of an exhaustive number of membrane-, cell wall-, and transport-related genes, which is probably related with its effect on membrane permeability (3). Furthermore, the increase in the number of genes differentially expressed in response to *bolA* overexpression between 1 h and 3 h suggests a gradual response leading to additional indirect regulations, possibly involving more than one pathway (such as through other regulators).

Together, the data obtained allowed us to observe that BolA is a versatile transcription factor able to either repress or induce gene expression both in early and late growth stages of *E. coli*. BolA has a wide spectrum of action, with consequences for the expression of many important genes.

BolA, an important *E. coli* protein in the switch between motile and sedentary lifestyles. Bacterial motility and chemotaxis help cells to reach favorable environments and to successfully compete with other microorganisms in response to external stimuli (19, 20). Our results indicate an accentuated downregulation of genes involved in flagellar biosynthesis 1 h after *bolA* induction (Fig. 1B). More specifically, our data show a differential regulation of the transcripts encoding FlhD and FlhC, two proteins that together function as the master transcriptional regulators of flagellar synthesis (21). The expression of these two genes was reduced more than 2-fold (ratio of *bolA*++ to Δ*bolA* is <0.5) in the presence of elevated levels of BolA. Reduced expression of *flhD* and *flhC* upon BolA induction was confirmed by RT-PCR (see Fig. S2A). Consistent with this observation, four flagellum-associated genes (*flgB*, *fliN*, *flgE*, *flgC*) were significantly downregulated (Table 1). Moreover, 33% of the flagellar genes were associated with expression ratios lower than 0.66, suggesting widespread downregulation of this cellular mechanism (see Fig. S2B). Given BolA is involved in the downregulation of flagellar genes, we wanted to test its overall role in *E. coli* motility control. For this, bacterial swimming capacity was tested (Fig. 2A). Three different strains (see Table S1 in the supplemental material for strain and plasmid details) expressing BolA at different levels, standard expression (wild type [wt]), constitutive overexpression from a medium-copy-number plasmid (*bolA*+ strain), and an even higher overexpression obtained with an arabinose induction system, the same used in the array expression study described above (*bolA*++ strain), were used in this analysis. The *bolA*+ strain is an MG1655 strain carrying the plasmid pMAK580 (medium-copy-number plasmid) that was originally used as a noninducible plasmid to overproduce BolA under the control of its own promoters (1). After 26 h of growth, all strains, except the *bolA*++ strain, covered the whole plate. The wt showed higher motility than the strain moderately overexpressing *bolA* (*bolA*+

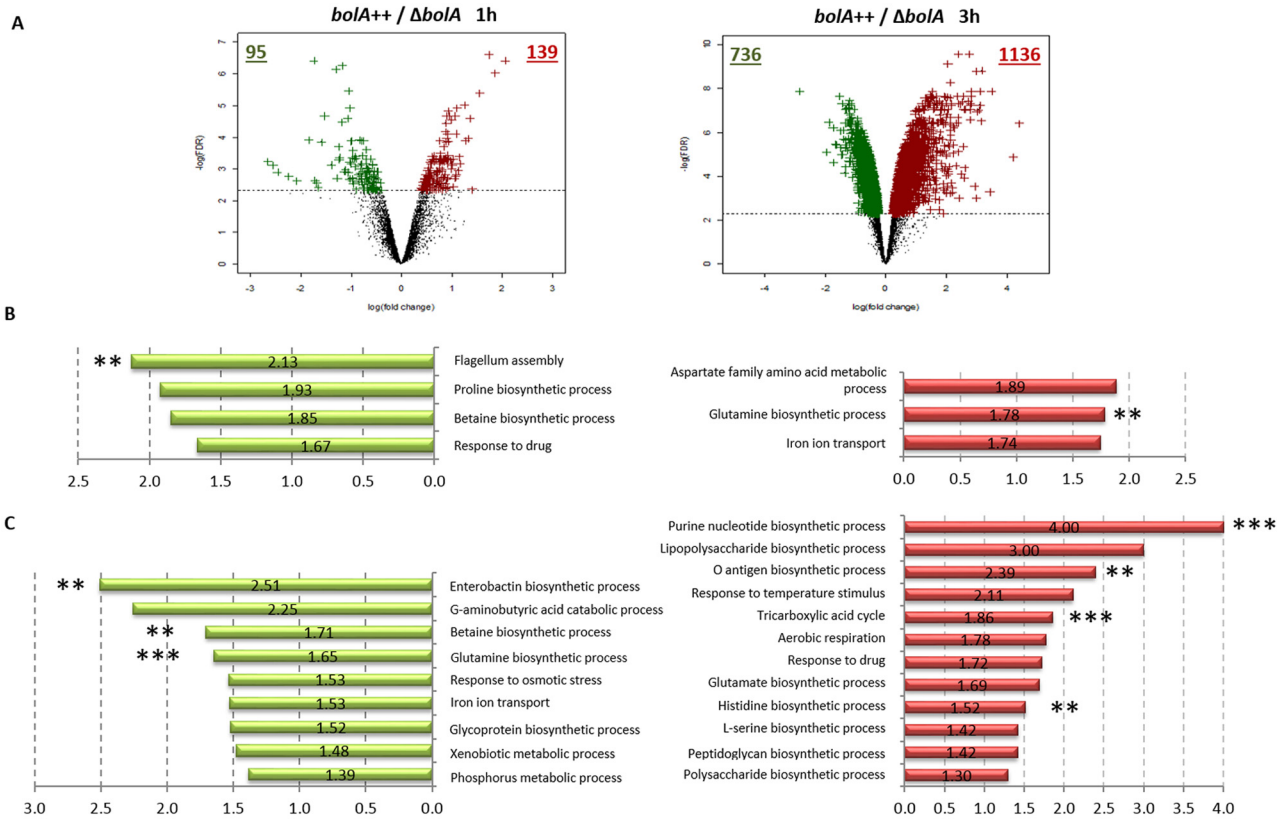

FIG 1 Classification and graphical representation of the transcriptome assay. (A) Volcano plots representing the transcriptome results corresponding to the time point of 1 h (left side) and 3 h (right side) after *bolA* induction. Genes associated to an FDR lower than 10% (represented by the dashed horizontal line) were considered significant. The green and red spots represent the downregulated and upregulated genes. The numbers of genes significantly repressed or overexpressed under each condition are indicated by the green and red numbers, respectively. (B) Graphical representation of the gene ontology (GO) biological process enrichments results 1 h after *bolA* induction. Functional categories that were significantly overrepresented among upregulated or downregulated genes are shown. Bar length corresponds to the average fold change (in absolute value of the *bolA*++/Δ*bolA* ratio) of the genes significantly upregulated or downregulated associated with each GO category according to transcriptome results. (C) Graphical representation of GO biological process enrichment results 3 h after *bolA* induction with the respective fold change (*bolA*++/Δ*bolA*). The asterisk represents the statistical significance level of the differential expression of each GO category. Green graphic shows downregulated genes and red the upregulated genes. **, *P* value associated with the enrichment test was lower than 5×10^{-4}; ***, *P* value associated with the enrichment test was lower than 5×10^{-6}. No asterisk indicates that the *P* value associated with the enrichment test was between 5×10^{-2} and 5×10^{-4}.

strain). The *bolA*+ strain, even with less motility capacity, is still able to swim more efficiently than the strain overexpressing *bolA* at high levels (*bolA*++ strain). Thus, in agreement with the downregulation of flagellum-associated genes, higher levels of BolA lead to reduced motility. This confirms that the BolA protein is repressing the expression of flagellar genes with consequences in the swimming capacity of bacteria. The effects on motility were not just observed at a given time point but were also registered and quantified during the time course of bacterial growth (Fig. 2B). The impact of BolA on motility together with the downregulation of several flagellar genes suggested the existence of an impairment during the synthesis of the flagella or a negative mechanical effect on its structure/rotation. According to the transcriptome, the expression of *ycgR*, a gene encoding a protein that can control bacterial swimming velocity (22), seems to be BolA independent. Thus, we decided to perform immunofluorescence to confirm flagellar presence in our conditions (Fig. 2C). A wt strain was used as a positive control presenting several flagella per bacterial cell. However, when we analyzed the *bolA*+ and *bolA*++ strains, the flagella were not clearly observed. Therefore, the swimming im-

TABLE 1 Differentially regulated genes involved in different pathways of bacterial metabolism[a]

Gene	Fold change	*P* value
Flagellar pathway genes (1 h after induction)		
flgB	*4.54*	$9.36E^{-03}$
fliN	*2.63*	$6.67E^{-02}$
flgE	*2.70*	$2.07E^{-02}$
flgC	*3.57*	$6.72E^{-02}$
Pyruvate metabolism genes (3 h after induction)		
ppsA	**1.48**	$9.44E^{-02}$
aceE	**1.67**	$9.75E^{-03}$
aceF	**1.58**	$1.57E^{-02}$
TCA cycle genes (3 h after induction)		
gltA	**1.71**	$4.34E^{-02}$
sucA	**4.81**	$2.62E^{-03}$
sdhA	**2.48**	$3.35E^{-02}$

[a] Represented in Table 1 is the fold change of the *bolA*++/Δ*bolA* ratio for several genes responsible for the expression of proteins involved in the flagellar synthesis pathway, pyruvate, and TCA cycle metabolisms. The italic and bold numbers indicate the downregulated and upregulated genes, respectively. The *P* value associated with each gene represents the statistical significance level of the differential expression.

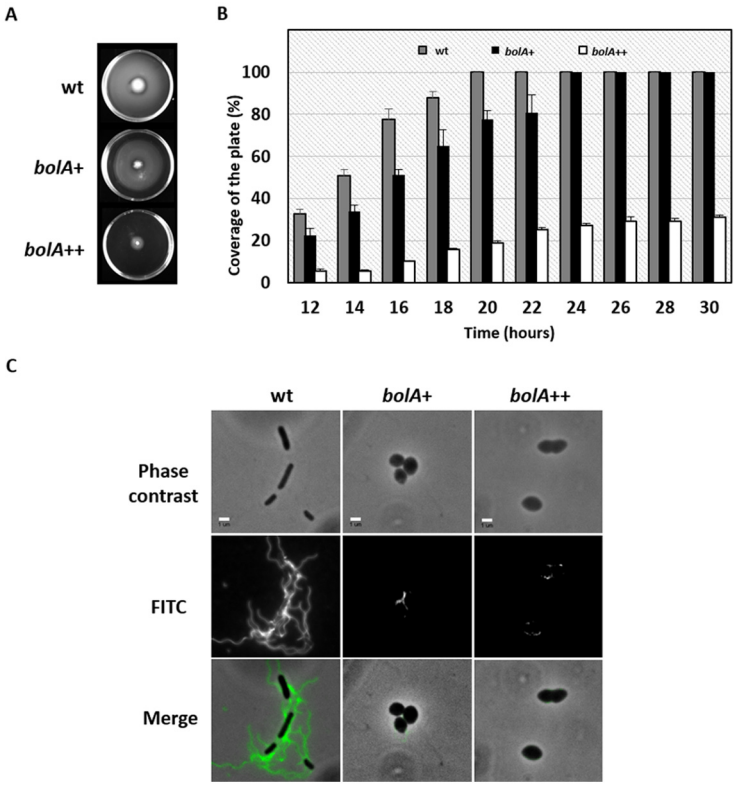

FIG 2 Motility assays in the presence of different doses of BolA protein. (A) To measure motility, bacteria were inoculated in swimming agar plates. The plates were incubated at 37°C for 18 h and photographed. (B) Time course analysis of the bacterial swimming. The dispersion radius was quantified between 12 h and 26 h of incubation at 37°C. One-hundred percent represents the detection limit (whole plate covered by the swimming halo). (C) Observation of *E. coli* flagella using immunofluorescent staining with antiflagellin antibody. Scale bar represents 2 μm.

pairment is not a simple delay in flagellar movement but a problem of flagellar assembly.

Elevated levels of BolA induce the expression of TCA cycle enzymes. Our results show a variety of enzymes involved in metabolic pathways being differentially regulated in the presence of elevated levels of BolA (Table 1). Figure S3 in the supplemental material gives a graphical overview of metabolic pathways affected by BolA. Glycolysis and the pentose phosphate pathway do not seem to be modulated by BolA. However, many genes linked to pyruvate metabolism (*ppc*, *ppsA*, *aceE*, *lpd*, *mqo*, *qckA*, *aceF*, *acs*) and the tricarboxylic acid (TCA) cycle (*gltA*, *aceB*, *ybhJ*, *icd*, *sucA*, *sucB*, *sucC*, *sucD*, *sdhA*, *sdhB*, *sdhC*, *sdhD*, *fumA*) are induced upon *bolA* overexpression. The TCA cycle plays a central role in metabolism. Many nutrients, like sugars, amino acids, and fatty acids, can be metabolized into TCA intermediates (23). Interestingly, the increased level of genes involved in oxidative phosphorylation (*nuoBCEFGHIJKLM*) can be directly related with an increased activity of the TCA cycle due to the maintenance of NAD(P)H/NAD(P)$^+$ cofactor balance in the cells. A general upregulation of several amino acid pathways, including glutamate, valine, lysine, and alanine, was also observed 3 h after *bolA* induction. The differential regulation of genes from other metabolic pathways is probably due to indirect regulations, although in a BolA-dependent manner.

Biofilm formation and matrix composition is influenced by BolA levels. TCA cycle activity has been associated with the production of biofilm components and polysaccharide intercellular adhesins (24, 25). Furthermore, different TCA cycle enzymes have been found to be upregulated in biofilm-grown cells compared to planktonic cells (26). It was previously shown for the *E. coli* MG1693 strain that the overexpression of BolA leads to increased biofilm formation (4). This biofilm assay was reproduced here using the four strains expressing different levels of BolA in the MG1655 genetic background (Δ*bolA*, wt, *bolA*+, and *bolA*++ strains). The results are presented in Fig. 3A and corroborate the previous findings showing that BolA favors biofilm formation.

Fimbriae are one of the essential structures necessary for the initial step of biofilm formation (27), helping the adhesion process of the bacteria to surfaces. Surprisingly, the transcriptome results do not show a significant variation on the expression of genes related with type I fimbriae upon *bolA* overexpression. However, 3 h after BolA induction, there is a remarkable overexpression of several genes encoding fimbria-like adhesins (*ydeS*, *yadC*, *yraH*, *yehD*, *ygiL*, *yadK*, *yadN*, *ybgD*, *yfcV*, *yehC*, *yadM*), which is very likely sufficient to increase the adhesion capacity of the *bolA*++ strain. This observation was also visible at the phenotypic level, since scanning electron microscopy revealed the presence of several fimbria-like structures when BolA intracellular levels are elevated (Fig. 3B).

Together with fimbriae, lipopolysaccharides (LPS), the main component of the *E. coli* outer membrane, are believed to play a role in the bacterial adhesion to abiotic surfaces (28). The overexpression of BolA led to an increase in the levels of genes associated with LPS biosynthesis. More specifically, the *rfaQGPSBIJYZK*

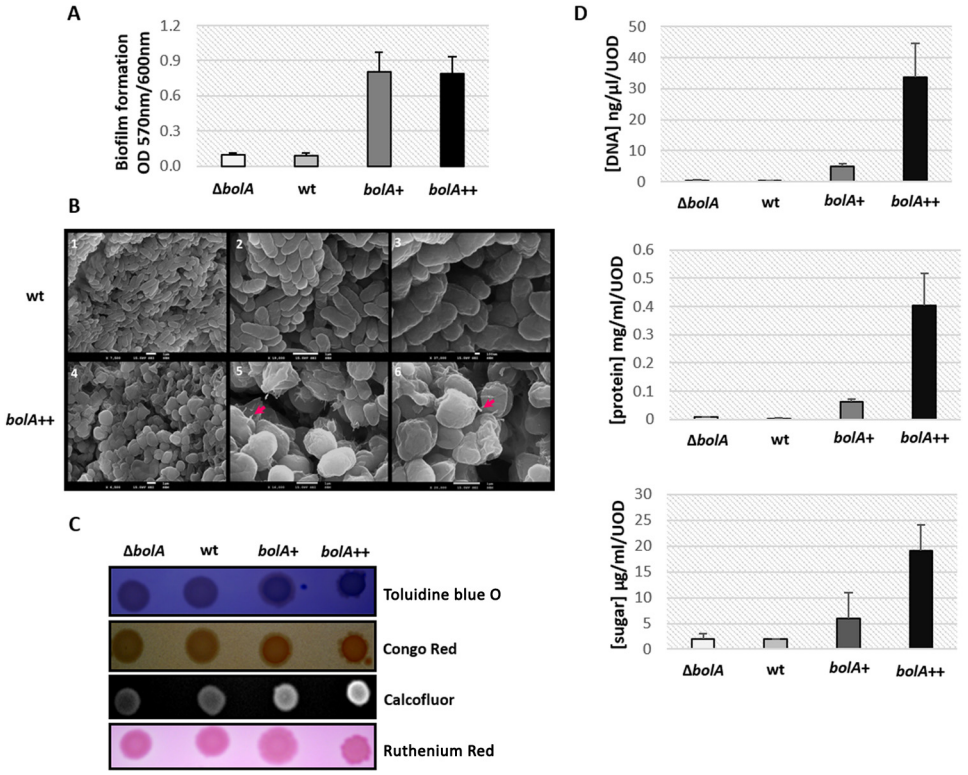

FIG 3 Influence of the BolA protein in bacterial structures and extracellular components involved in biofilm matrix formation. (A) Effect of BolA on biofilm development in microtiter plates. The thickness of biofilms in cultures of different strains was measured by determining the OD_{570} after staining with crystal violet and normalization by OD_{600} of the planktonic culture. Error bars represent standard deviations. (B) Scanning electron microscopy images of the wt and *bolA*++ strains. Images were obtained from overpopulated LB plates supplemented with arabinose. The secondary imaging mode of scanning electron microscopy was used. Panels 1 to 3 correspond to wt, while 4 to 6 correspond to the *bolA*++ strain. The wt displays the regular *E. coli* bacillus shape, whereas the characteristic BolA overexpression-associated round phenotype can be observed in *bolA*++ images. The arrows indicate the observed fimbria-like adhesins produced by the bacterial cells in the presence of elevated levels of BolA. (C) A blue color on the toluidine blue O plate indicates the production of extracellular DNA (eDNA). In Congo red plates, the brown, dry, and rough (BDAR) phenotype reveals the production of curli, while the red, dry, and rough (RDAR) phenotype indicates the presence of both curli and cellulose. Regarding the Calcofluor plates, fluorescence detection is indicative of polysaccharide (such as cellulose) production. Finally, a pink color in ruthenium red plates stands for the presence of colanic acid production. (D) Quantification of extracellular sugar, DNA, and protein produced by the different strains expressing BolA after 18 h of growth on an LB plate at 37°C.

operon, which encodes mainly enzymes that modify LPS structure (29), was entirely and strongly upregulated, with an average factor of 4.52 times. On the other hand, *rfaH*, which is known to repress biofilm formation (30), is the only *rfa* gene found to be downregulated by BolA, strengthening the role of BolA in the promotion of biofilm communities.

To further investigate the role of BolA in biofilms, the production of extracellular components associated with the biofilm matrix was assayed. Using appropriated dyes on LB agar plates, the different phenotypes among strains overexpressing *bolA* (*bolA*+ and *bolA*++ strains), the Δ*bolA* strain, and the wt could be observed (Fig. 3C). The presence of brown, dry, and rough (BDAR) colonies on Congo red plates is indicative of curli production in all the strains used in this work. Using Calcofluor plates, a fluorochrome that binds to (1-3)-β- and (1-4)-β-D-glucopyranosides (31), it was possible to observe binding to this fluorochrome. Although *E. coli* K-12 is described to not bind Calcofluor due to a mutation in the *bcsA* gene, which has consequences for cellulose production (32, 33), the strains overexpressing BolA were notably and reproducibly brighter, which indicates a significantly higher production of polysaccharides than the wt or Δ*bolA* strain. This phenotype is strongly supported at the transcriptomic level by the remarkable upregulation of genes involved in polysaccharides, such as those responsible for cellulose biosynthesis, in the presence of BolA. The operon *bscEFG* is indeed significantly upregulated 1 h and 3 h after *bolA* induction. Furthermore, exopolysaccharides were also assessed using a medium containing ruthenium red, and we observed a positive effect on the production of these sugars in the presence of BolA.

Extracellular DNA (eDNA) and proteins are two additional components of the extracellular matrix extremely important to encase bacteria to the surfaces (34). To assess whether the production of eDNA was correlated with BolA overexpression, cells were grown on toluidine blue O plates. The strains overexpressing *bolA* were darker blue, meaning that they produced more eDNA, which correlates with the transcriptomic activation of genes related to purine and pyrimidine metabolism. To further complete this analysis, the differences in eDNA production were quantified in bacteria cultured in LB overnight (Fig. 3D). Similarly to what was observed on toluidine blue O plates, the total eDNA produced increased concomitantly with the increasing BolA levels, being able to reach a difference of up to 45-fold-higher levels than those of the wt. Proteins and exopolysaccharides were quantified in a similar way. Their amounts also increased in the presence of ele-

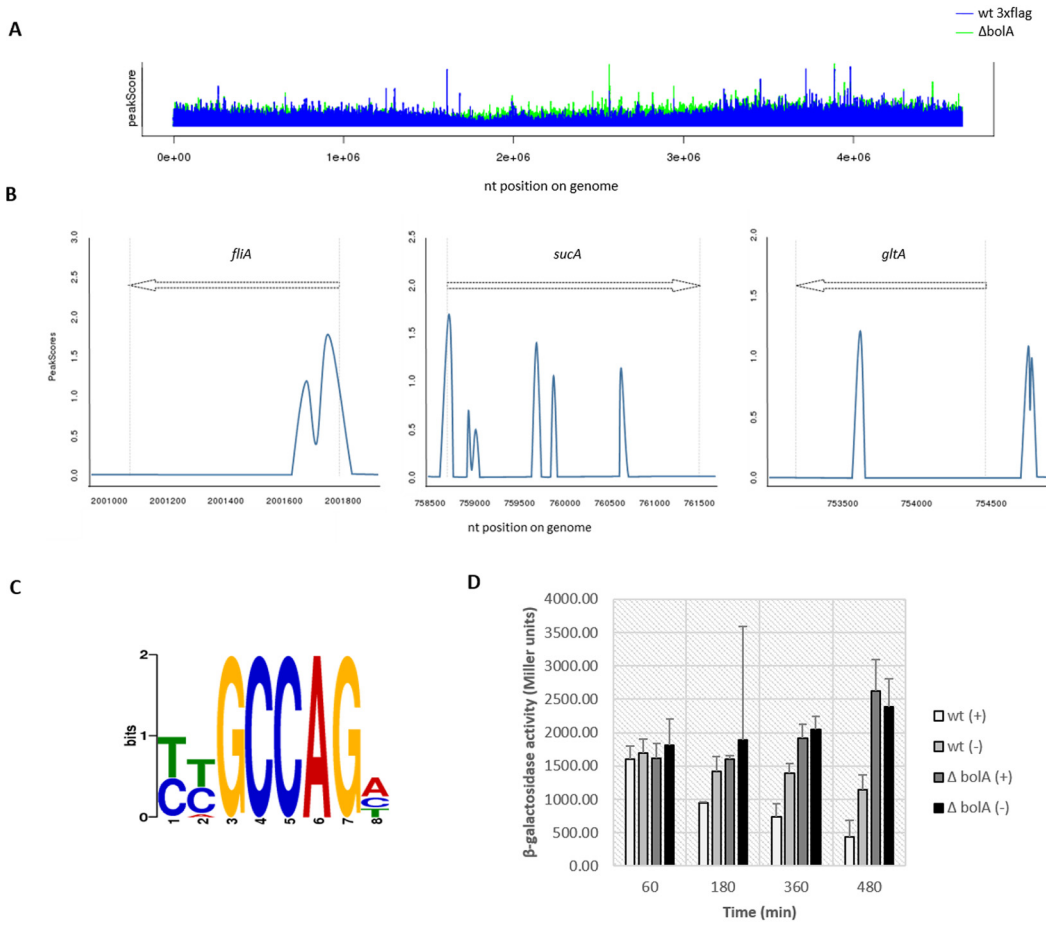

FIG 4 Graphical representation of the BolA ChIP-seq results, DNA consensus sequence, and its effect on the transcription of downstream genes. (A) Statistically significant peaks detected for wt 3×Flag and Δ*bolA* strains. For data processing, the Δ*bolA* strain was considered the background and subtracted from the wt 3×Flag sample. (B) Graphical representation of the peaks associated with three different targets determined by ChIP-seq. BolA binding regions are spread in the chromosome, not only at the 5′ untranslated region (UTR), but also along the ORFs. (C) The BolA consensus was determined based on the pool of DNA sequences corresponding to the identified peaks. The statistical significance of the consensus obtained is associated with a *P* value of 6.1×10^{-3}. (D) Graphic showing the β-galactosidase activity of a construct with the *mreBCD* promoter region containing the consensus sequence and a second construct without it. The plus sign represents the extracts where the consensus was present, while the minus sign indicates the absence of the consensus. The experiment was performed in the wt and the Δ*bolA* backgrounds. In agreement with the BolA-dependent *mreB* downregulation, when the consensus sequence is not present, an increased activity of β-galactosidase can be observed, strengthening the importance of the consensus for the proper BolA-dependent regulation. Additionally, in the Δ*bolA* background, there are no significant differences between the two extracts, excluding the hypothesis of a construct-dependent effect.

vated levels of BolA. The release of extracellular material can probably be linked with the already described effects of BolA in bacterial membrane alteration and permeability (1, 3, 15, 16). According to our transcriptomic data, 50% of the genes coding for membrane-associated proteins together with 40% of the genes coding for transporters are differentially regulated. These results correlate with the significant cell membrane and morphology alterations that can be observed by electron microscopy (Fig. 3B). The transcriptomic analysis together with the functional enrichment analysis further revealed the significant upregulation of genes coding for proteins involved in peptidoglycan biosynthesis.

Together, these observations highlight the link between BolA and the attachment/biofilm matrix processes in *E. coli*.

BolA is a transcription factor directly interacting with specific regions of the genome. In order to further characterize the role of this protein, we tested whether BolA was directly acting as a transcription factor in the regulation of the genes previously mentioned. Chromatin immunoprecipitation followed by DNA high-throughput sequencing (ChIP-seq) was performed to determine the genome-wide binding ability of BolA. For this purpose, two *E. coli* strains were used: a strain where the *bolA* gene was deleted (Δ*bolA* strain) and an isogenic strain carrying a chromosomal fusion of BolA with a 3×Flag tag (wt 3×Flag). The strain containing the 3×Flag tag was assessed for alterations on the function of the BolA protein *in vivo*. To validate the use of this construct, morphology and growth curves were analyzed, and they were confirmed to be similar to a wt strain (see Fig. S4A and B in the supplemental material). Both the Δ*bolA* and wt 3×Flag strains were grown to exponential phase followed by chromatin immunoprecipitation with a Flag-specific antibody. Sequencing of all the precipitated nucleic acids allowed the statistical identification of DNA-enriched sequences. Our results indicate that BolA is able to bind directly in a statistically significant manner to different regions of the *E. coli* chromosome (Fig. 4A). The analyses were carried with a false discovery rate (FDR) of 0.1, resulting in approximately 1,300 peaks identified. The binding regions are

TABLE 2 Affinity measurement with bio-layer interferometry[a]

Protein	Analyte	K_D	K_a (1/Ms)	K_a error	K_d (1/s)	K_d error
BolA	*fliA*	$5.67E^{-08}$	$1.35E^{04}$	$4.91E^{02}$	$7.63E^{-04}$	$5.16E^{-05}$
	gltA	$5.02E^{-08}$	$3.74E^{04}$	$2.14E^{03}$	$1.88E^{-03}$	$2.36E^{-04}$
	mreBCD	$9.34E^{-08}$	$5.69E^{04}$	$2.15E^{03}$	$5.32E^{-03}$	$2.51E^{-04}$
	flhDC	ND	ND	ND	ND	ND
	Random oligonucleotide	ND	ND	ND	ND	ND
BSA	*mreBCD*	ND	ND	ND	ND	ND

[a] Equilibrium constants (K_D) were determined by bio-layer interferometry using the BLItz system (ForteBio Inc.) according to an advanced kinetics experiment. K_a is the association rate constant, K_d the dissociation rate constant, and K_D the equilibrium dissociation constant of the reaction. ND, not determined.

spread in the chromosome and located not only at the 5′-end untranslated regions (UTR) but also inside the open reading frames (ORFs) (Fig. 4B). Among the targets identified were the *mreB* and *ampC* genes, previously identified as transcriptionally dependent of BolA (15, 17). To validate our ChIP-seq results, direct interactions of the BolA protein with several DNA targets were successfully confirmed in real time by bio-layer interferometry (Table 2). For this purpose, we overexpressed and purified the BolA protein by liquid chromatography, and we analyzed its binding to the selected DNA sequences corresponding to different BolA affinity regions identified in the ChIP-seq assay. Our results not only validated the ChIP-seq data but also confirmed the ability of this protein to directly interact with nucleic acids *in vitro*. Direct binding was observed in genes present in diverse functional categories. Hypergeometric tests were performed on the groups of genes significantly overrepresented in the BolA-precipitated DNA fraction. This test aims at identifying the enrichment in functional categories as defined in GO and/or KEGG pathway classifications. In agreement to what was previously observed at the transcriptional level, the flagellar assembly, peptidoglycan biosynthesis, and tricarboxylic acid (TCA) cycle GO categories were among the significant overrepresented targets. While the impact of BolA at the mRNA level of regulation of flagellum-related genes observed in the transcriptome was already significant (including the regulation of about 33% of the genes involved in the flagellar synthesis pathway [see Fig. S2B]), ChIP-seq results showed that BolA is directly regulating 45% of the differentially expressed genes belonging to the flagellar cascade. Figure 5 represents flagellar structure and related proteins containing the microarrays and the ChIP-seq results. The red boxes stress the genes in which BolA was directly binding according to ChIP-seq results. In green are the genes downregulated. Our results indeed indicate an interaction of BolA with the DNA sequences corresponding to genes encoding flagellar transcription regulators (*fliA*, *fliZ*), genes encoding proteins that compose the flagellar basal body (*flgC*, *fliF*, *fliG*, *fliN*, *fliM*) and hook (*flgD*, *flgJ*), and even those involved in hook-filament junction (*flgK*, *flgL*).

As previously mentioned, even without a direct effect of BolA in the two major carbon metabolism pathways (glycolysis and pentose phosphate pathways), TCA cycle enzymes were observed to be significantly modulated in a BolA-dependent manner. This fact was further strengthened by the direct binding of BolA to several genes encoding these enzymes. While several identified targets correlate well with the regulation of mRNA expression after 1 h and 3 h of *bolA* induction, there are others which vary only in one or the other condition used. For instance, the genes related to the TCA cycle (*gltA*, *ybjJ*, *icd*, *sucA*, *sucB*, *sucC*, *sdhB*, *sdhC*) appear to be significantly increased after only 3 h of induc-

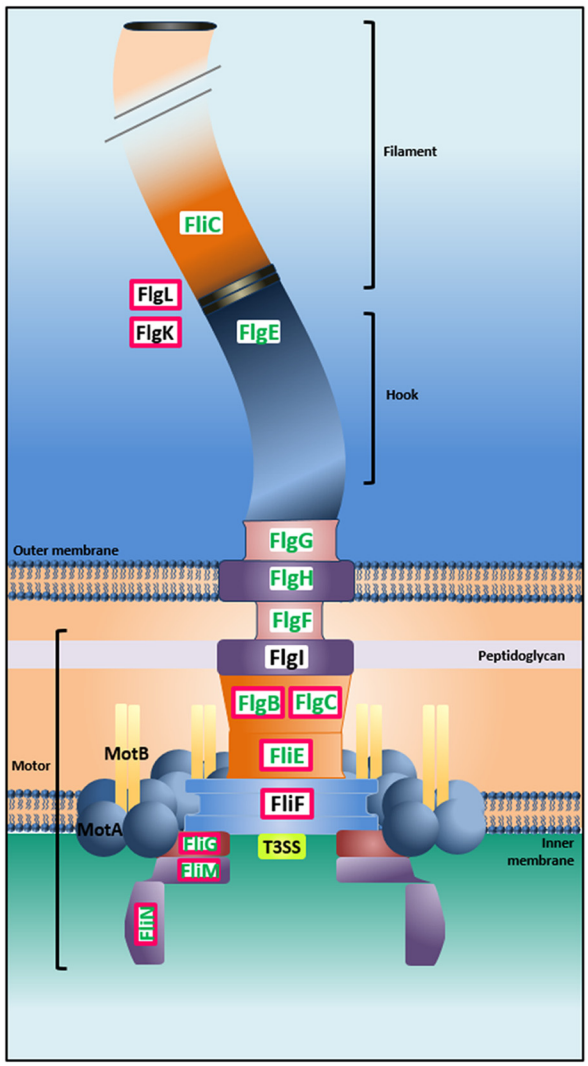

FIG 5 Representative flagellar structure and related proteins coupled with microarrays and ChIP-seq analysis results. ChIP-seq analysis showed the capacity of BolA to directly interact with different genes encoding proteins involved in diverse steps of the flagellar biosynthesis pathway. Of the 33% negatively regulated genes related with the flagellar structure (*bolA*++/Δ*bolA* ratios), 45% were identified as direct BolA targets (the proteins in pink boxes are encoded by the target genes). The proteins highlighted in green correspond to the respective downregulated genes. Additionally to the genes indicated in the figure, *fliZ*, *fliA*, *flgD*, and *flgJ* were also found to be direct targets of BolA.

tion. Similarly, some GO categories appeared enriched only in one of the two conditions studied. Enrichment of the sequences corresponding to *rfaH*, a gene required for the production of extracellular components such as lipopolysaccharide (35), was observed, supporting the role of BolA in the direct regulation of LPS metabolism at the transcription level.

Finally, all sequences corresponding to the identified peaks were used to perform a bioinformatics determination of the consensus protein-DNA binding region. Different motif search software was implemented. When the results obtained with the different tools were compared, a consensus sequence with an associated *P* value of 6.1×10^{-3} was identified (Fig. 4C). The veracity of the consensus was validated by inverted motif search using Regulatory Sequencing Analysis Tools (RSAT) DNA pattern matching software. The YYGCCAGH nucleotide sequence was used as a query search against the 5′ end of the entire coding region of the *E. coli* genome. The experiment was carried out allowing zero or one mismatch. When zero mismatches were allowed, 22.6% of BolA direct targets presented the tested sequence, while only 5% of the entire genome coding regions were positive for the presence of the consensus. Moreover, when one mismatch was allowed, it was possible to detect in 39.5% of the whole-genome coding regions the consensus sequence previously found, while for the total BolA direct targets, 78.9% were positive for this sequence. Thus, the percentage of genes with the requested motif was found to be lower in the whole genome than in the set of genes significantly identified in the ChIP-seq experiment.

In order to evaluate the impact of the consensus in the transcriptional rate of downstream genes, we have performed transcriptional fusions of β-galactosidase with a promoter containing the consensus core (GCCAG) or without it. The promoter sequence used corresponds to the *mreBCD* promoter. The β-galactosidase activity of the two different extracts was compared, and the results can be observed in Fig. 4D. In early exponential phase of growth (60 min), significant differences in Miller units were not observed between the different constructs. However, when middle exponential phase (180 min), early stationary phase (360 min), or late stationary phase are reached, changes in β-galactosidase activity are noticeable. When the correct sequence of the consensus is present, Miller units reduced up to 60%, depending on the growth phase of the bacteria. These results are in agreement with the BolA repressor activity over this promoter, as shown previously (17). Additionally, this reduction is strictly related with BolA activity due to the absence of differences in β-galactosidase activity in the Δ*bolA* background.

In brief, we have shown that BolA is an important transcription factor, with a specific preferred DNA binding motif, which is involved in the regulation of flagellar biosynthesis, TCA cycle, and peptidoglycan synthesis.

DISCUSSION

BolA has been described as a protein important for survival in late stages of bacterial growth and under harsh environmental conditions (2, 3). High levels of BolA in stationary phase and stress have been connected with a plethora of phenotypes, strongly suggesting its important role as a master regulator (18). In this report, we have investigated the role of BolA as a transcription factor at a global level. We have used ChIP-seq technology to produce the first chromosome-wide direct analysis of DNA binding *in vivo* by *E. coli* BolA. Our results show that BolA directly binds to a significant number of gene sequences, from the 5′-end region to the open reading frames. Moreover, even though a blurred asymmetry in read densities between strands was observed, BolA seems to behave more as a transcription factor than a nucleoid-associated protein. The blurred effect may be related to complexes that this protein possibly form when interacting with the DNA. These results firmly support the role of BolA as a transcription factor, as suggested in previous studies (16, 17). BolA was previously associated with positive and negative regulation of gene expression (15, 17), an observation that prompted us to examine the overall transcription in the bacterial cells. Transcriptome analysis confirmed the dual role of BolA as an activator or a repressor of transcription.

ChIP-seq and transcriptome data suggest BolA direct effects are related to the repression of flagellum-associated genes and the induction of genes related with the TCA cycle. Both flagellar and TCA cycle genes have direct consequences on bacterial motility (25, 36). Flagella and motility have been the center of research attention of many research groups due to their roles in virulence and biofilm development (22, 27, 37). The remarkable effect of the presence of elevated levels of BolA in the regulation of flagellar biosynthesis and TCA cycle enzymes was observed not only at the transcriptional level but also at the phenotypic level. With the overexpression of BolA, a reduction of the swimming capacity of *E. coli* was observed. The gradual reduction of the bacterial swimming capacity concomitantly with the increment of BolA strongly suggests a dose effect of this protein. This observation shows cells must exercise tight control over BolA levels.

The reduction of swimming can be associated with a variety of mechanisms, and the two most studied are the assembly and the rotation of flagella (38). Our results suggest BolA affects the assembly of flagella. We indeed observe a repression of genes which are flagellar transcriptional regulators and several others that encode the hook proteins and the hook filament junction proteins. Additionally, using immunofluorescence, in the strains overexpressing BolA, the flagella were practically not detected, conversely to what was observed in the wt, supporting the role of BolA in flagellar repression.

Flagella are required for the initial stages of biofilm formation in *E. coli* (39). Even though there is a reduction in flagellar biosynthesis with the concomitant overexpression of BolA, it is plausible to hypothesize that the presence of adhesins could significantly contribute to this process, since flagellar motility was described to be dispensable for the initial adhesion in strains overexpressing adhesins (40). In this regard, the reduced motility of the strains overexpressing BolA was most likely compensated by the overexpression and production of fimbria-like adhesins. Moreover, under the conditions tested, there are evidences of differential regulation of an elevated number of genes associated with LPS biosynthesis, polysaccharide production, and membrane-associated enzymes. It was described that *E. coli* K-12 does not produce cellulose due to a mutation in the *bcsA* gene (32, 33). However, our strains overproducing BolA showed the characteristic Calcofluor binding phenotype. This could indicate binding to other exopolysaccharides, such as colanic acid or poly-1,6-GlcNAc (PGA). Furthermore, extracellular DNA, protein, and sugar levels were all augmented in the overexpression strain compared to those in the wt condition. Noticeably, all the components mentioned above are important for the assembly and composition of the biofilm matrix, which protects bacteria in the biofilm com-

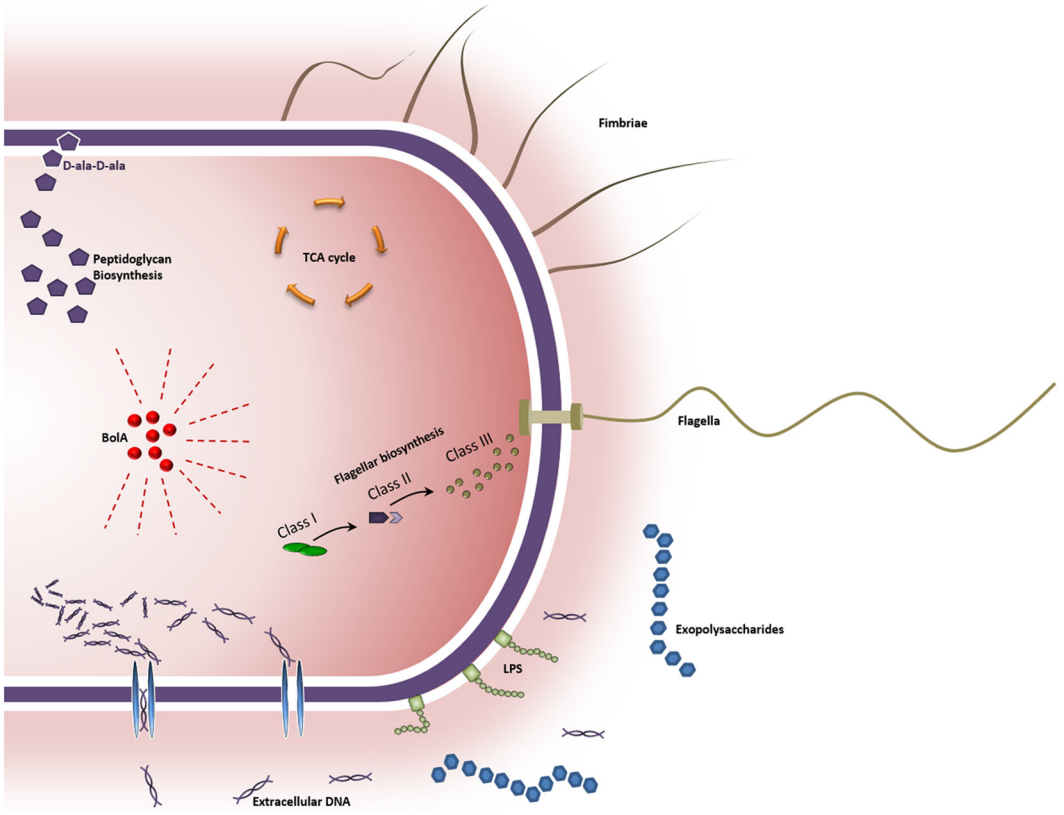

FIG 6 Model for BolA-mediated regulation of planktonic-to-sessile transition-related mechanisms in *Escherichia coli*. BolA is a global regulator which has a major direct effect in bacterial motility through the repression of flagellum-associated genes and the induction of tricarboxylic acid (TCA) cycle genes. It modulates the regulation of several carbon metabolism pathways connected to peptidoglycan biosynthesis. Biofilm formation is favored by BolA mainly through the differential regulation of genes involved in lipopolysaccharide (LPS) and cellulose production. The presence of elevated levels of extracellular DNA, proteins, and sugars emphasizes the role of this protein in the production of an extracellular matrix necessary for biofilm development. Concordantly, BolA induction has a positive effect in the expression of several genes encoding fimbria-like adhesins, which are possibly involved in the formation of the three-dimensional structure of biofilms.

munity (28, 34). Work previously performed in our lab has shown that in *E. coli*, BolA expression is correlated with the capacity to form biofilm (4). These new results have significantly contributed to understanding the mechanism by which BolA overexpression contributes to biofilm formation and to extending the role of BolA to other related pathways. For instance, our results showed BolA directly inhibits the expression of *ompX*, a gene whose inactivation has a positive effect on the initial step of adhesion mediated by fimbriae (41). BolA mediates the induction of the cold shock regulators *cspABFGI*, which were previously shown to positively regulate the first hours of biofilm formation (42). Similarly, deletions in respiratory genes such as *hyaACD* were shown to increase biofilm formation (42), and in fact our results indicate BolA represses the *hyaABCDEF* operon.

The overall regulation of central carbon metabolism by BolA includes the induction of genes related to several amino acid pathways and the direct activation of the transcription of several of the TCA cycle enzymes. Together, all these regulations are connected to biofilm formation mechanisms through peptidoglycan biosynthesis (see Fig. S3 in the supplemental material). The genes upregulated at the transcriptional level 3 h after BolA induction are connected with the synthesis of peptidoglycan, a major biofilm component (43). BolA also modulates additional cellular pathways which connect to the synthesis of peptidoglycan via a number of intermediate metabolic networks, as highlighted in Fig. S3 (in red metabolic pathways upregulated in the *bolA++* strain). This interconnection is reinforced by the predicted upregulation of the TCA cycle within biofilms (44, 45).

In order to further characterize the mode of action of the BolA protein and determine a consensus DNA binding motif, an *in silico* analysis was performed using a pool of sequences obtained with the ChIP-seq assay. Three different motifs were obtained; however, two of them were present only in 8 and 6 of the total number of sequences tested. The third motif was in 92 of these sequences and thus considered the statistically significant consensus region for the BolA protein (TC)(TC)GCCAG(ACT). This represents a major breakthrough in the characterization of this recently discovered *E. coli* transcription factor, allowing to further characterize the mode of action of this protein and study the interaction with its targets. Furthermore, STRING database (46) and text-mining data indicate the possible *in vivo* interaction of BolA with other *E. coli* transcription factors, including σ^S and H-NS. The question of BolA binding exclusively on its own or in synergy with another protein hence remains open.

Biofilm formation is a well-studied but extremely complex process. It involves five different stages and a panoply of cellular structures and components (47). The various surface structures determinant in each step of *E. coli* biofilm formation have been

summarized and listed (27). Briefly, initial adhesion requires flagella and motility. Type I fimbriae, curli and exopolysaccharides are involved in the second stage. In the third stage, curli, antigen Ag43, exopolysaccharides, and colanic acid have an essential role. Finally, curli and colanic acid additionally participate in the late maturation together with conjugative pili before dispersal is accomplished thanks to flagella and motility. BolA overexpression favors biofilm formation and involves production of fimbria-like adhesins and curli together with the increment of colanic acid production.

In summary, BolA is an important transcription factor able to directly repress or induce gene expression and is involved in the regulation of flagellar biosynthesis, TCA cycle, and peptidoglycan synthesis. In Fig. 6, we represent a model with the major impacts of BolA in the bacterial cell. This work constitutes a relevant step toward the comprehension of BolA protein and will have important applications for homologues in other organisms, namely, in biofilm-producing pathogenic bacteria. BolA belongs to a family of proteins that are widely conserved from prokaryotes to eukaryotes (48). Although their exact function is not fully established at the molecular level, they seem to be involved in cell proliferation and cell cycle regulation. Herein, we propose that BolA is a very important motile/adhesive transcriptional switch, specifically involved in the transition between the planktonic and the attachment stage of the biofilm formation process. Together, the molecular studies of different lifestyles coupled with the comprehension of the BolA functions may be an important breakthrough for future perspectives, with major health care and biotechnology applications.

MATERIALS AND METHODS

Bacterial growth conditions. *E. coli* was cultivated in Luria Bertani broth (LB) at 37°C with agitation, unless differently specified. When appropriate, antibiotics were used at the following concentrations: 100 μg/ml ampicillin, 50 μg/ml kanamycin, 20 μg/ml tetracycline, 50 μg/ml chloramphenicol. Luria agar plates as well as M9 minimal medium plates were used and supplemented with arabinose 0.15% when necessary.

Oligonucleotides, bacterial strains, and plasmids. Restriction enzymes, T4 DNA ligase, *Pfu* DNA polymerase, and T4 polynucleotide kinase were purchased from Fermentas. All enzymes were used according to the supplier's instructions. Strains and plasmids are listed in Table S1 in the supplemental material. All oligonucleotides used in this work are listed in Table S2 and were synthesized by STAB Vida.

E. coli strain DH5α was used for cloning experiments. P1-mediated transduction to transfer the desired mutations to the wt strain was performed as previously described (49). Plasmids were transformed into electro- or chemo-competent (50) *E. coli* cells.

In order to express BolA in *trans*, the wt *bolA* coding sequence was obtained by PCR amplification with primers BolAFwNcoI and X9-KpnI. The resulting PCR product was digested with NcoI and KpnI and cloned into the pBAD vector previously cleaved with the same restriction enzymes and named pCDA2. For the *mreB* promoter cloning, primers pairs RNM213/RNM214 and RNM215/RNM214 were used to obtain the PCR product with the correct consensus and with the modified consensus, respectively. Both fragments were digested with SmaI and SalI and cloned into the pSP417 vector previously cleaved with the same restriction enzymes. These constructions were named pSBA01 and pSBA02, respectively.

The λRed-mediated mutagenesis method (51) was used to obtain the wt 3×Flag and Δ*ycgR* strains. Briefly, for the wt 3×Flag strain, a PCR fragment was obtained by amplification of pSUB11 (52) plasmid using the primers rnm112 and rnm114. The resulting fragment was transformed in AB330-competent cells to allow recombination with the bacterial chromosome. The recombinant strains were used for P1 transduction to the wt strain. All constructs were confirmed by DNA sequencing at STAB Vida, Portugal.

Overexpression and purification of the BolA protein. BolA overexpression using the pPFA02 plasmid and protein purification was performed as previously described (16). The plasmid used for expression of BolA was a pET28a-derived pPFA02 (17) transformed into a Novagen *E. coli* BL21(DE3) strain. Purification of BolA was performed by histidine affinity chromatography using HisTrap chelating HP columns (GE Healthcare) and an AKTA fast protein liquid chromatography system (GE Healthcare).

RNA extraction. Overnight cultures were diluted 1/100 in fresh LB medium and grown until an OD_{600} of approximately 0.4 before the addition of 0.15% arabinose to induce BolA expression. Culture samples were collected 1 h and 3 h after the induction, and total RNA was extracted as previously described (2).

Microarrays. The quality of the RNA was assessed with a Bioanalyzer (Agilent Technology). RNA was processed for use on the GeneChip *E. coli* genome 2.0 array from Affymetrix according to the manufacturer's protocol. Hybridization, scanning, and detection procedures were done at the Genomics Unit of the Instituto Gulbenkian de Ciência (Portugal).

Subsequent exploration, normalization, summarization, and analyses of the generated Affymetrix CEL files were performed using R open source statistical software (http://cran.r-project.org/) and its associated tool for high-throughput genomic data, Bioconductor (http://www.bioconductor.org/). The reliability of the data set, before and after normalization, was estimated through its statistical exploration.

Statistical analysis of differentially regulated genes. The empirical Bayes statistics was used to analyze the data, providing a robust estimate of variance for each gene. The multiple testing issue was further taken into account through the calculation of the FDR according to the Benjamini-Hochberg method (53). Genes displaying a *bolA*++/Δ*bolA* ratio associated with an FDR lower than 10% were considered differentially regulated. It was checked that the *t*-statistic *P* value was lower than 5%, with mean of values of 0.11 and 1.01% for the comparison 1 h and 3 h after BolA induction, respectively.

RT-PCR. RT-PCR reactions were performed as previously described (13). The primer pairs flgB_qPCR-1/flgB_qPCR-2, rnm166/rnm167, flhD001/flhD_Probe, flhC001/flhC_Probe, fliA_qPCR-1/fliA_qPCR-2, rnm156/rnm157, and rnm158/rnm159 were used to analyze *flgB*, *hdfR*, *flhD*, *flhC*, *fliA*, *icd*, and *gltA* expression, respectively.

ChIP-seq. The Δ*bolA* and wt 3×Flag strains were used to perform ChIP-seq experiments. Overnight cultures were diluted 1/100 in fresh LB medium and grown until an OD_{600} of 0.6. A total of 10 mM of sodium phosphate and formaldehyde to a final concentration of 1% were then added. Cross-linked cells were harvested and washed with ice-cold phosphate-buffered saline (PBS). Cells were resuspended in TES buffer (50 mM Tris-HCl [pH 7.5], 150 mM NaCl) and lysis solution (13.6 mg/ml lysozyme, 50% glycerol, 50 mM Tris-HCl [pH 7.5], 100 mM NaCl, 1 mM dithiothreitol [DTT], 0.1% Triton X-100), followed of a 5-min incubation at room temperature. Ten microliters of cOmplete EDTA-free protease inhibitor (Roche) was added and incubated for 10 min at room temperature. ChIP buffer (1.1% Triton X-100, 1.2 mM EDTA, 16.7 mM Tris-HCl, 167 mM NaCl, 20 μl/ml of cOmplete EDTA-free protease inhibitor) was added, followed by a 10-min incubation at 37°C. The lysate was then sonicated (UP200S-Hielscher), insoluble cell debris was removed by centrifugation, and the supernatant was collected. The supernatant was added to anti-Flag agarose beads (Sigma) and incubated at 4°C under rotation. The samples were then washed with successive salt-based buffers, from a low to a high salt concentration, followed by a wash with LiCl buffer and TE buffer. Two additional washes with freshly prepared elution buffer (1% SDS, 100 mM $NaHCO_3$) were done, followed by vortexing and incubation under rotation at room temperature for 15 min. To reverse the cross-link, 5 M NaCl was added to the elute and incubated overnight at 65°C. Finally, 0.5 M EDTA, 1 M Tris-HCl (pH 6.5), and 10 mg/ml protei-

nase K (Sigma) were added, and the suspension was incubated at 45°C for 2 h. DNA was purified and recovered by standard phenol-chloroform extraction and ethanol precipitation with 20 μg of glycogen.

Library construction, sequencing, and statistical analysis were performed by Fasteris SA, Switzerland. The alignment was done using BWA software and the Peak detection using SeqMonk and CLC genomics software.

Determination of dissociation constant. The dissociation constant (K_D) of the interaction of BolA with the different substrates was determined using the BLItz system (ForteBio Inc.) according to the user instructions and was calculated as dissociation rate (K_d) divided by association rate (K_a). Biotin-labeled DNA fragments were obtained by PCR. The primers rnm019/rnm188, rnm153/rnm186, rnm193/rnm194, and rnm190/mreBrev were used to amplify the promoter regions of *flhD*, *fliA*, *gltA*, and *mreBCD*, respectively. Three different concentrations of protein were used for kinetics measurement corresponding to 500 nM, 1,000 nM, and 1,500 nM purified BolA protein. A negative control with a random DNA sequence was performed as well as a bovine serum albumin (BSA) protein assay.

Consensus binding motif search. The search of a DNA consensus binding motif for BolA was carried out based on the peak sequences obtained in the ChIP-seq experiment. The defined set of sequences for motif search (about 1,300 different sequences) was processed in MEME-ChIP software (54) with default parameters and prokaryote or *E. coli* as the input motif database. The consensus BolA binding motif was further confirmed using other motif search software, such as RSAT oligo-analysis (55), CompleteMOTIFs (56), ChIPMunk (57), and DREME (58). Additionally, the determined sequence was tested by inverted motif search using RSAT DNA pattern matching software (59).

β-Galactosidase activity assay. β-Galactosidase activity assays were performed as described previously (60) with some modifications. Briefly, bacterial cells were precipitated by centrifugation and resuspended in buffer A (60 mM $Na_2HPO_4{\cdot}7H_2O$, 40 mM $NaH_2PO_4{\cdot}H_2O$, 10 mM KCl, 1 mM $MgSO_4$, and 50 mM β-mercaptoethanol, pH 7.0). The OD_{600} of the suspension was measured, and then a volume of cells was mixed with buffer B (4 mg/ml in 100 mM phosphate buffer [pH 7.0]). The reaction was carried until a yellow color was observed, and the reaction was stopped with the addition of a stop solution (1 M Na_2CO_3). The suspension was centrifuged, and the OD_{420} and OD_{550} of the supernatant were determined. The equation Miller units = $1{,}000 \times (OD_{420} - (1.75 \times OD_{550}))/(t \times v \times OD_{600})$ was used to determine the units of enzyme activity.

Immunofluorescent staining of flagella. Glass coverslips were incubated in a 1:10 poly-L-lysine solution (Sigma) for 5 min and were allowed to dry at 50°C for 60 min. Bacteria were fixed with a 4% paraformaldehyde (Sigma) solution followed by incubation at room temperature for 15 min. Cells were pipetted to the previously coated poly-L-lysine glass coverslips and incubated for 10 min at room temperature. The preparations were blocked in 1× PBS containing 4% BSA for 45 min. The coverslips were then incubated with a rabbit polyclonal antiflagellin antibody (Abcam) for 60 min. After three washes with 1× PBS, the samples were incubated for 45 min with monoclonal anti-rabbit immunoglobulin-fluorescein isothiocyanate (FITC) antibody (Sigma). The samples were washed three times and mounted onto glass slides using 4 μl of Prolong (Molecular Probes). Images were acquired using a Leica dm6000 B fluorescence microscope coupled with a Leica CTR6000 electronics box.

Bright-field phase microscopy. Planktonic cells were harvested from cultures growing in LB at the selected time points. Cells were fixed with 0.75% (vol/vol) formaldehyde and stored at 4°C. For the differential interference contrast (DIC) microscopy photographs, samples were observed in slides coated with a thin 1.5% (wt/vol) agarose film and enclosed with a no. 1 cover glass. Images were obtained using a DMRA microscope (Leica, Wetzlar, Germany) under Nomarski optics coupled to a charge-coupled-device camera, with Metamorph software.

Scanning electron microscopy. Cells were fixed for 2 h in 3% glutaraldehyde in 0.1 M sodium cacodylate buffer (pH 7.3), followed by a washing step, and then fixed in 1% osmium tetroxide in the same buffer. After incubation in hexamethyldisilazane (HMDS), drops of the bacterial suspension were applied to a glass coverslip, dried, and covered with chromium in a Quantum Q150T sputter coater. Cells were observed and photographed in a JEOL 7001F FEG-SEM.

Swimming motility assays. Fresh swimming plates were prepared with swimming medium (10 g/liter tryptone, 5 g/liter NaCl, 0.15% arabinose, 0.3% agar), dried for 15 min, and inoculated with bacterial culture in exponential phase. Plates were incubated at 37°C, and pictures were taken regularly using the Chemidoc Imaging system (BioRad). ImageJ software was used to measure the diameter of the swimming halo (results are normalized by the diameter of the plates).

Biofilm assays. Overnight cultures grown in LB were diluted to a final OD_{600} of ~0.1 in fresh M9 medium. A 200-μl aliquot of the diluted culture was added to each well of a 96-well polystyrene microtiter plate (Sarstedt). Plates were incubated at 37°C without shaking for 24 h. Planktonic growth was determined by measuring the OD_{600} in a spectrophotometer (Eppendorf). The plates were washed twice with double-distilled water (ddH_2O), and any bacteria retained in the biofilm were stained with 0.1% crystal violet. The crystal violet was solubilized by the addition of a solution of acetone-ethanol (1:4), and the estimation of biofilm density was determined by measuring the OD_{570} and normalizing by OD_{600}.

Quantification of extracellular material. Bacterial cells were resuspended in 0.9% NaCl, and OD_{600} was measured. Bacterial suspension was centrifuged for 10 min at maximum speed, and the supernatant was collected. Two and a half times the volume of supernatant of 99% cold ethanol was added to the tubes. Samples were centrifuged for 20 min at 4°C and maximum speed. The resulting pellet was dried overnight at 65°C. The dried pellet was resuspended in ddH_2O. NanoDrop 1000 (NanoDrop Technologies) was used to measure protein and DNA concentrations in the samples. For EPS (exopolysaccharide) quantification, a dilution of 1/10 of each sample was prepared. Diluted samples were mixed with a phenol solution (5 g phenol in H_2O). To the mixture, sulfuric acid reagent was added (2.5 g hydrazine sulfate in 500 ml sulfuric acid). Samples were vortexed and incubated for ~1 h at 4°C before absorbance was read at 490 nm. The concentrations were determined according to a glucose calibration curve. Final values of DNA, protein, and EPS were normalized by the initial measured OD_{600}.

Extracellular-component-associated phenotype characterization. Ten microliters of cells in exponential phase of growth was inoculated in LB agar plates supplemented with 150 μg/ml Congo red, 40 μg/μl toluidine blue O, 80 μg/μl Calcofluor, or 40 μg/ml ruthenium red. When required, 0.15% arabinose was added. All plates were incubated for 18 h at 37°C.

Microarray data accession number. The ChIP-seq data from this publication have been submitted to the Gene Expression Omnibus (GEO) database and assigned the identifier accession number GSE58623. The microarray identifier accession number is GSE58509.

SUPPLEMENTAL MATERIAL

Supplemental material for this article may be found at http://mbio.asm.org/lookup/suppl/doi:10.1128/mBio.02352-14/-/DCSupplemental.

Figure S1, TIF file, 2.2 MB.
Figure S2, TIF file, 2.4 MB.
Figure S3, TIF file, 0.9 MB.
Figure S4, TIF file, 2.6 MB.
Table S1, PDF file, 0.03 MB.
Table S2, DOCX file, 0.02 MB.

ACKNOWLEDGMENTS

We thank Urs Jenal for the experimental advice and critical reading of the manuscript, Andreia Aires for technical assistance, Alberto Reinders for helping with the ChIP-seq assay, and Arsénio M. Fialho for help with the extracellular material quantification method.

R.N.M. (postdoctoral fellow), C.D. (postdoctoral fellow), and S.B. (research fellow) received fellowships from FCT-Fundação para a Ciência e Tecnologia, Portugal. This work was supported by grants from Fundação para a Ciência e a Tecnologia, Portugal, including R.N.M. postdoctoral grant SFRH/BPD/84080/2012, PTDC/QUI-BIQ/111757/2009, PTDC/BIA-MIC/4142/2012, PEst-OE/EQB/LA0004/2013, and European Commission grant FP7-KBBE-2011-1-289326.

REFERENCES

1. **Aldea M, Hernández-Chico C, de la Campa AG, Kushner SR, Vicente M.** 1988. Identification, cloning, and expression of *bolA*, an *ftsZ*-dependent morphogene of *Escherichia coli*. J Bacteriol **170:**5169–5176.
2. **Santos JM, Freire P, Vicente M, Arraiano CM.** 1999. The stationary-phase morphogene *bolA* from *Escherichia coli* is induced by stress during early stages of growth. Mol Microbiol **32:**789–798. http://dx.doi.org/10.1046/j.1365-2958.1999.01397.x.
3. **Freire P, Vieira HL, Furtado AR, de Pedro MA, Arraiano CM.** 2006. Effect of the morphogene *bolA* on the permeability of the *Escherichia coli* outer membrane. FEMS Microbiol Lett **260:**106–111. http://dx.doi.org/10.1111/j.1574-6968.2006.00307.x.
4. **Vieira HL, Freire P, Arraiano CM.** 2004. Effect of *Escherichia coli* morphogene *bolA* on biofilms. Appl Environ Microbiol **70:**5682–5684. http://dx.doi.org/10.1128/AEM.70.9.5682-5684.2004.
5. **Adnan M, Morton G, Singh J, Hadi S.** 2010. Contribution of *rpoS* and *bolA* genes in biofilm formation in *Escherichia coli* K-12 MG1655. Mol Cell Biochem **342:**207–213. http://dx.doi.org/10.1007/s11010-010-0485-7.
6. **Koch B, Nybroe O.** 2006. Initial characterization of a *bolA* homologue from *Pseudomonas fluorescens* indicates different roles for BolA-like proteins in *P. fluorescens* and *Escherichia coli*. FEMS Microbiol Lett **262:**48–56. http://dx.doi.org/10.1111/j.1574-6968.2006.00359.x.
7. **Khona DK, Dongre SS, Arraiano CM, D'Souza JS.** 2013. A *bolA*-like morphogene from the alga *Chlamydomonas reinhardtii* changes morphology and induces biofilm formation in *Escherichia coli*. FEMS Microbiol Lett **339:**39–47. http://dx.doi.org/10.1111/1574-6968.12051.
8. **Freire P, Amaral JD, Santos JM, Arraiano CM.** 2006. Adaptation to carbon starvation: RNase III ensures normal expression levels of *bolA1p* mRNA and sigma(s). Biochimie **88:**341–346. http://dx.doi.org/10.1016/j.biochi.2005.09.004.
9. **Lange R, Hengge-Aronis R.** 1991. Identification of a central regulator of stationary-phase gene expression in *Escherichia coli*. Mol Microbiol **5:**49–59. http://dx.doi.org/10.1111/j.1365-2958.1991.tb01825.x.
10. **Santos JM, Freire P, Mesquita FS, Mika F, Hengge R, Arraiano CM.** 2006. Poly(A)-polymerase I links transcription with mRNA degradation via sigmas proteolysis. Mol Microbiol **60:**177–188. http://dx.doi.org/10.1111/j.1365-2958.2006.05078.x.
11. **Aldea M, Garrido T, Hernández-Chico C, Vicente M, Kushner SR.** 1989. Induction of a growth-phase-dependent promoter triggers transcription of *bolA*, an *Escherichia coli* morphogene. EMBO J **8:**3923–3931.
12. **Yamamoto K, Nagura R, Tanabe H, Fujita N, Ishihama A, Utsumi R.** 2000. Negative regulation of the *bolA1p* of *Escherichia coli* K-12 by the transcription factor OmpR for osmolarity response genes. FEMS Microbiol Lett **186:**257–262. http://dx.doi.org/10.1111/j.1574-6968.2000.tb09114.x.
13. **Moreira RN, Dressaire C, Domingues S, Arraiano CM.** 2011. A new target for an old regulator: H-NS represses transcription of *bolA* morphogene by direct binding to both promoters. Biochem Biophys Res Commun **411:**50–55. http://dx.doi.org/10.1016/j.bbrc.2011.06.084.
14. **Arraiano CM, Andrade JM, Domingues S, Guinote IB, Malecki M, Matos RG, Moreira RN, Pobre V, Reis FP, Saramago M, Silva IJ, Viegas SC.** 2010. The critical role of RNA processing and degradation in the control of gene expression. FEMS Microbiol Rev **34:**883–923. http://dx.doi.org/10.1111/j.1574-6976.2010.00242.x.
15. **Santos JM, Lobo M, Matos AP, De Pedro MA, Arraiano CM.** 2002. The gene *bolA* regulates *dacA* (PBP5), *dacC* (PBP6) and *ampC* (AmpC), promoting normal morphology in *Escherichia coli*. Mol Microbiol **45:**1729–1740. http://dx.doi.org/10.1046/j.1365-2958.2002.03131.x.
16. **Guinote IB, Matos RG, Freire P, Arraiano CM.** 2011. BolA affects cell growth, and binds to the promoters of penicillin-binding proteins 5 and 6 and regulates their expression. J Microbiol Biotechnol **21:**243–251. http://dx.doi.org/10.4014/jmb.1009.09034.
17. **Freire P, Moreira RN, Arraiano CM.** 2009. BolA inhibits cell elongation and regulates MreB expression levels. J Mol Biol **385:**1345–1351. http://dx.doi.org/10.1016/j.jmb.2008.12.026.
18. **Guinote IB, Moreira RN, Barahona S, Freire P, Vicente M, Arraiano CM.** 2014. Breaking through the stress barrier: the role of BolA in Gram-negative survival. World J Microbiol Biotechnol **30:**2559–2566. http://dx.doi.org/10.1007/s11274-014-1702-4.
19. **Fenchel T.** 2002. Microbial behavior in a heterogeneous world. Science **296:**1068–1071. http://dx.doi.org/10.1126/science.1070118.
20. **Stocker R, Seymour JR, Samadani A, Hunt DE, Polz MF.** 2008. Rapid chemotactic response enables marine bacteria to exploit ephemeral microscale nutrient patches. Proc Natl Acad Sci U S A **105:**4209–4214. http://dx.doi.org/10.1073/pnas.0709765105.
21. **Macnab RM.** 1992. Genetics and biogenesis of bacterial flagella. Annu Rev Genet **26:**131–158. http://dx.doi.org/10.1146/annurev.ge.26.120192.001023.
22. **Boehm A, Kaiser M, Li H, Spangler C, Kasper CA, Ackermann M, Kaever V, Sourjik V, Roth V, Jenal U.** 2010. Second messenger-mediated adjustment of bacterial swimming velocity. Cell **141:**107–116. http://dx.doi.org/10.1016/j.cell.2010.01.018.
23. **Gaupp R, Schlag S, Liebeke M, Lalk M, Götz F.** 2010. Advantage of upregulation of succinate dehydrogenase in *Staphylococcus aureus* biofilms. J Bacteriol **192:**2385–2394. http://dx.doi.org/10.1128/JB.01472-09.
24. **Somerville GA, Chaussee MS, Morgan CI, Fitzgerald JR, Dorward DW, Reitzer LJ, Musser JM.** 2002. *Staphylococcus aureus* aconitase inactivation unexpectedly inhibits post-exponential-phase growth and enhances stationary-phase survival. Infect Immun **70:**6373–6382. http://dx.doi.org/10.1128/IAI.70.11.6373-6382.2002.
25. **Vuong C, Kidder JB, Jacobson ER, Otto M, Proctor RA, Somerville GA.** 2005. *Staphylococcus epidermidis* polysaccharide intercellular adhesin production significantly increases during tricarboxylic acid cycle stress. J Bacteriol **187:**2967–2973. http://dx.doi.org/10.1128/JB.187.9.2967-2973.2005.
26. **Resch A, Rosenstein R, Nerz C, Götz F.** 2005. Differential gene expression profiling of *Staphylococcus aureus* cultivated under biofilm and planktonic conditions. Appl Environ Microbiol **71:**2663–2676. http://dx.doi.org/10.1128/AEM.71.5.2663-2676.2005.
27. **Van Houdt R, Michiels CW.** 2005. Role of bacterial cell surface structures in *Escherichia coli* biofilm formation. Res Microbiol **156:**626–633. http://dx.doi.org/10.1016/j.resmic.2005.02.005.
28. **Beloin C, Roux A, Ghigo JM.** 2008. *Escherichia coli* biofilms. Curr Top Microbiol Immunol **322:**249–289. http://dx.doi.org/10.1007/978-3-540-75418-3_12.
29. **Raetz CR, Whitfield C.** 2002. Lipopolysaccharide endotoxins. Annu Rev Biochem **71:**635–700. http://dx.doi.org/10.1146/annurev.biochem.71.110601.135414.
30. **Beloin C, Michaelis K, Lindner K, Landini P, Hacker J, Ghigo JM, Dobrindt U.** 2006. The transcriptional antiterminator RfaH represses biofilm formation in *Escherichia coli*. J Bacteriol **188:**1316–1331. http://dx.doi.org/10.1128/JB.188.4.1316-1331.2006.
31. **Weiner L, Model P.** 1994. Role of an *Escherichia coli* stress-response operon in stationary-phase survival. Proc Natl Acad Sci U S A **91:**2191–2195. http://dx.doi.org/10.1073/pnas.91.6.2191.
32. **Da Re S, Ghigo JM.** 2006. A CsgD-independent pathway for cellulose production and biofilm formation in *Escherichia coli*. J Bacteriol **188:**3073–3087. http://dx.doi.org/10.1128/JB.188.8.3073-3087.2006.
33. **Serra DO, Richter AM, Klauck G, Mika F, Hengge R.** 2013. Microanatomy at cellular resolution and spatial order of physiological differentiation in a bacterial biofilm. mBio **4**(2):e00103-00113. http://dx.doi.org/10.1128/mBio.00103-13.
34. **Flemming HC, Wingender J.** 2010. The biofilm matrix. Nat Rev Microbiol **8:**623–633. http://dx.doi.org/10.1038/nrmicro2415.
35. **Beutin L, Manning PA, Achtman M, Willetts N.** 1981. *sfrA* and *sfrB* products of *Escherichia coli* K-12 are transcriptional control factors. J Bacteriol **145:**840–844.
36. **Wood TK, González Barrios AF, Herzberg M, Lee J.** 2006. Motility influences biofilm architecture in *Escherichia coli*. Appl Microbiol Biotechnol **72:**361–367. http://dx.doi.org/10.1007/s00253-005-0263-8.
37. **Duan Q, Zhou M, Zhu L, Zhu G.** 2013. Flagella and bacterial pathogenicity. J Basic Microbiol **53:**1–8. http://dx.doi.org/10.1002/jobm.201100335.
38. **Jarrell KF, McBride MJ.** 2008. The surprisingly diverse ways that prokaryotes move. Nat Rev Microbiol **6:**466–476. http://dx.doi.org/10.1038/nrmicro1900.

39. **Pratt LA, Kolter R.** 1998. Genetic analysis of *Escherichia coli* biofilm formation: roles of flagella, motility, chemotaxis and type I pili. Mol Microbiol **30:**285–293. http://dx.doi.org/10.1046/j.1365-2958.1998.01061.x.
40. **Prigent-Combaret C, Prensier G, Le Thi TT, Vidal O, Lejeune P, Dorel C.** 2000. Developmental pathway for biofilm formation in curli-producing *Escherichia coli* strains: role of flagella, curli and colanic acid. Environ Microbiol **2:**450–464. http://dx.doi.org/10.1046/j.1462-2920.2000.00128.x.
41. **Otto K, Hermansson M.** 2004. Inactivation of *ompX* causes increased interactions of type 1 fimbriated *Escherichia coli* with abiotic surfaces. J Bacteriol **186:**226–234. http://dx.doi.org/10.1128/JB.186.1.226-234.2004.
42. **Domka J, Lee J, Bansal T, Wood TK.** 2007. Temporal gene-expression in *Escherichia coli* K-12 biofilms. Environ Microbiol **9:**332–346. http://dx.doi.org/10.1111/j.1462-2920.2006.01143.x.
43. **Karatan E, Watnick P.** 2009. Signals, regulatory networks, and materials that build and break bacterial biofilms. Microbiol Mol Biol Rev **73:**310–347. http://dx.doi.org/10.1128/MMBR.00041-08.
44. **Mukherjee J, Ow SY, Noirel J, Biggs CA.** 2011. Quantitative protein expression and cell surface characteristics of *Escherichia coli* MG1655 biofilms. Proteomics **11:**339–351. http://dx.doi.org/10.1002/pmic.201000386.
45. **Prüss BM, Verma K, Samanta P, Sule P, Kumar S, Wu J, Christianson D, Horne SM, Stafslien SJ, Wolfe AJ, Denton A.** 2010. Environmental and genetic factors that contribute to *Escherichia coli* K-12 biofilm formation. Arch Microbiol **192:**715–728. http://dx.doi.org/10.1007/s00203-010-0599-z.
46. **Jensen LJ, Kuhn M, Stark M, Chaffron S, Creevey C, Muller J, Doerks T, Julien P, Roth A, Simonovic M, Bork P, von Mering C.** 2009. String 8—a global view on proteins and their functional interactions in 630 organisms. Nucleic Acids Res **37:**D412–D416. http://dx.doi.org/10.1093/nar/gkn760.
47. **Stoodley P, Sauer K, Davies DG, Costerton JW.** 2002. Biofilms as complex differentiated communities. Annu Rev Microbiol **56:**187–209. http://dx.doi.org/10.1146/annurev.micro.56.012302.160705.
48. **Huynen MA, Spronk CA, Gabaldón T, Snel B.** 2005. Combining data from genomes, Y2H and 3D structure indicates that BolA is a reductase interacting with a glutaredoxin. FEBS Lett **579:**591–596. http://dx.doi.org/10.1016/j.febslet.2004.11.111.
49. **Sambrook J, Russell D.** 2001. Molecular cloning, a laboratory manual, 3rd ed. Cold Spring Harbor Laboratory Press, New York, NY.
50. **Inoue H, Nojima H, Okayama H.** 1990. High efficiency transformation of *Escherichia coli* with plasmids. Gene **96:**23–28. http://dx.doi.org/10.1016/0378-1119(90)90336-P.
51. **Datsenko KA, Wanner BL.** 2000. One-step inactivation of chromosomal genes in *Escherichia coli* K-12 using PCR products. Proc Natl Acad Sci U S A **97:**6640–6645. http://dx.doi.org/10.1073/pnas.120163297.
52. **Uzzau S, Figueroa-Bossi N, Rubino S, Bossi L.** 2001. Epitope tagging of chromosomal genes in salmonella. Proc Natl Acad Sci U S A **98:**15264–15269. http://dx.doi.org/10.1073/pnas.261348198.
53. **Benjamini Y, Drai D, Elmer G, Kafkafi N, Golani I.** 2001. Controlling the false discovery rate in behavior genetics research. Behav Brain Res **125:**279–284. http://dx.doi.org/10.1016/S0166-4328(01)00297-2.
54. **Machanick P, Bailey TL.** 2011. MEME-ChIP: motif analysis of large DNA datasets. Bioinformatics **27:**1696–1697. http://dx.doi.org/10.1093/bioinformatics/btr189.
55. **Van Helden J, André B, Collado-Vides J.** 1998. Extracting regulatory sites from the upstream region of yeast genes by computational analysis of oligonucleotide frequencies. J Mol Biol **281:**827–842. http://dx.doi.org/10.1006/jmbi.1998.1947.
56. **Kuttippurathu L, Hsing M, Liu Y, Schmidt B, Maskell DL, Lee K, He A, Pu WT, Kong SW.** 2011. CompleteMOTIFs: DNA motif discovery platform for transcription factor binding experiments. Bioinformatics **27:**715–717. http://dx.doi.org/10.1093/bioinformatics/btq707.
57. **Kulakovskiy IV, Boeva VA, Favorov AV, Makeev VJ.** 2010. Deep and wide digging for binding motifs in ChIP-Seq data. Bioinformatics **26:**2622–2623. http://dx.doi.org/10.1093/bioinformatics/btq488.
58. **Bailey TL.** 2011. DREME: motif discovery in transcription factor ChIP-seq data. Bioinformatics **27:**1653–1659. http://dx.doi.org/10.1093/bioinformatics/btr261.
59. **Thomas-Chollier M, Defrance M, Medina-Rivera A, Sand O, Herrmann C, Thieffry D, van Helden J.** 2011. RSAT 2011: regulatory sequence analysis tools. Nucleic Acids Res **39:**W86–W91. http://dx.doi.org/10.1093/nar/gkr377.
60. **Miller JH.** 1972. Experiments in molecular genetics. Cold Spring Harbor Laboratory Press, New York, NY.